Chapter 5 Structural Behaviour

E. Denarié, J. Silfwerbrand and H. Beushausen

Abstract Bonded cement-based material overlays and their substrates constitute a *hybrid or composite structural system*. The interaction of these two material layers (with different ages), with each other, with the external boundary conditions (foundations, supports) and possible joints, and under loading, defines the *structural behaviour* of this composite system.

The main *actions* governing this structural behaviour are (1) the differential deformations of the two layers due to autogenous shrinkage, thermo-mechanical effects due to cement hydration and/or external climatic influences and drying shrinkage, (2) settlements, and/or (3) imposed forces (dead loads, traffic loads). These actions give rise to stresses which depend on the stiffness of the substrate with respect to the new layer, and that eventually may result in failure either by transverse crack propagation, by debonding or both.

Composite structures formed of building materials of different kinds and ages are very common: slabs on grade, steel-concrete, wood-concrete, concrete-concrete, concrete repairs, cement-based overlays, etc. However, until now, the causes of distress in these composite structures and their design were mostly addressed by empirical approaches. This document shows how a common approach might treat all these applications on the unique basis of the mechanical description of the behaviour of composite structural members under restrained shrinkage.

MCS-IS-ENAC, Ecole Polytechnique Fédérale de Lausanne, Switzerland

Swedish Cement and Concrete Research Institute (CBI), SE-100 44 Stockholm, Sweden

H. Beushauser

Department of Civil Engineering, University of Cape Town, Rondebosch, South Africa

E. Denarié

J. Silfwerbrand

5.1 Introduction

Bonded cement-based material overlays and their substrates constitute a *hybrid or composite structural system*. The interaction under loading of these two material layers (with different ages), with each other and with the external boundary conditions (foundations, supports) and possible joints defines the *structural behaviour* of this composite system.

Composite structures formed of building materials of different kinds and ages are very common: slabs on grade, steel-concrete, wood-concrete, concrete-concrete, concrete repairs, cement-based overlays, etc. However, until now, the causes of distress in several of these composite structures and their design were mostly addressed by means of empirical approaches. This document shows how a common approach originally proposed by Silfwerbrand [1, 2] can treat all these applications on the unique basis of the mechanical description of the behaviour of composite structural members under restrained shrinkage.

Composite structural members are subjected to *actions* such as: (1) the differential deformations of the two layers due to autogenous shrinkage, thermo-mechanical effects due to cement hydration and/or external climatic influences and drying shrinkage, (2) settlements, and/or (3) imposed forces (dead loads, traffic loads). These actions give rise to stresses which depend on the stiffness of the substrate with respect to the new layer, and that eventually may result in failure either by transverse crack propagation, by de-bonding or both. The early age effects such as the thermo-mechanical effects are difficult to approximate with simplified approaches, due to the rapidly changing material properties.

There is a *complex interaction* between the structural behaviour and the modes of failure. If de-bonding can be prevented, the hybrid structure behaves in a *monolithic* way and structural failure will happen by transverse cracking. Otherwise, if debonding occurs, near cracks or joints, complex failure patterns can be obtained.

In the case of restrained deformations of the overlay, a simplified approach is to summarize the parameters related to the structure using the notion of *degree of restraint* of the overlay. Maximum restraint is obtained when all degrees of freedom (flexural and axial) of the overlay are blocked, i.e. the worst case scenario. The degree of restraint represents the *loading level* of the overlay with respect to maximum restraint. This approach has been investigated by several authors with the hypothesis of elastic materials. In the most general case, the structural response of a hybrid element can only be determined by a finite element simulation taking into consideration all relevant boundary conditions and material properties. The *viscoelastic behaviour* of the overlay, and if applicable, of the substrate, significantly contributes to the stress relaxation under imposed deformations. It can be taken into consideration by comprehensive numerical analyses, or by means of simplified analytical models.

Both the simplified approach based on the degree of restraint and the advanced numerical simulations can be used to *predict* the structural performance of composite systems, under imposed deformations of the overlay, with the *aim to select appropriate combinations of materials, thicknesses, reinforcements and joints.*

5.2 Actions

Note: The word "Actions" has to be understood here in a broad sense encompassing imposed forces and dead loads, as well as imposed displacements or deformations.

At early age and during their service life, overlays and composite members are subjected to various kinds of actions such as:

- Imposed deformations autogenous effects at early age, drying shrinkage, thermo-mechanical effects associated with hydration of binders (temperature gradients) at early age or to temperature gradients over the long term (see Chapter 3).
- *Imposed displacements* settlements, seismic loads.
- *Imposed forces* braking forces of vehicles, moving (fatigue) or gravity loads permanent loads in storage facilities (see Chapter 7).

The aim of this chapter is to provide an understanding of the mechanical behaviour in the case of restrained deformations of the overlay, rather than provide a comprehensive design method. A more detailed description of the deformations of overlay materials is given in Chapter 3. The overall actions to be considered for design as well as usual design methods are discussed in Chapter 7, for which this chapter can be seen as background.

5.3 Performance of Composite Structures

Composite structural components are formed of layers of different properties and age connected in a more or less monolithic way. The following applications belong to this category:

- steel-concrete composite constructions;
- partial replacement of existing concrete superstructures (kerbs on bridges);
- overlays on old concrete substrates (beams, slabs, columns);
- overlays on precast slabs; and
- pavements.

In the case of overlays, the overall performance of a composite system after the casting of a new layer on an existing substrate must be evaluated in the following terms:

- the protective function of the new layer and its serviceability; and
- the load-bearing capacity of the hybrid component and its behaviour at serviceability and ultimate (limit) state.

Figure 5.1, after Bernard [3], shows the evolution of the performance of a typical hybrid structural component formed of a new layer cast on an existing substrate. At early age, the partial restraint of the deformations of the new layer gives rise to

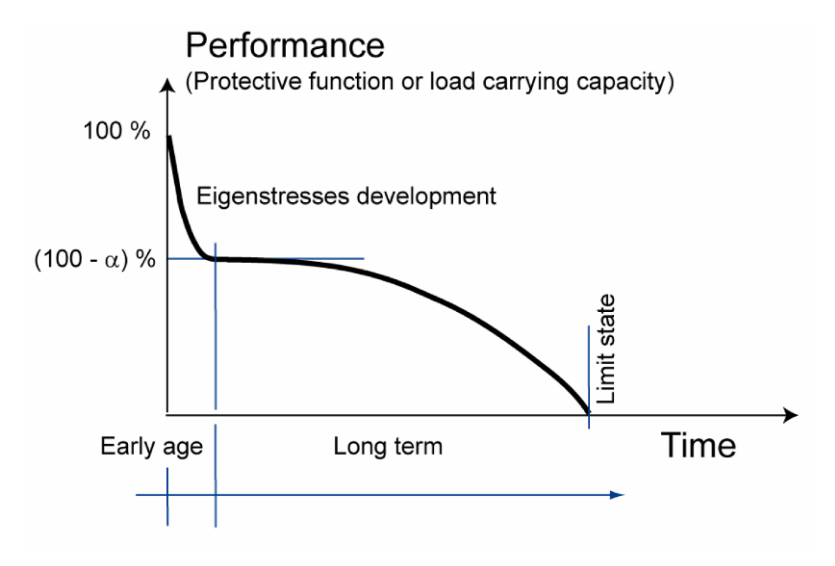


Fig. 5.1 Performance of composite structures [3]

eigenstresses that decrease with time due to the viscoelastic behaviour of the materials. The value of these eigenstresses can be considered as a "penalty" imposed on the intrinsic performance of the new layer, in terms of a reduction of the tensile stress that can be supported by this layer under service loads. This drop of the initial performance of the new layer must be taken into consideration in the calculation of the mechanical behaviour of the composite system. The mechanical behaviour of a composite structural member under loads can be calculated by means of simple well known theories from continuum mechanics and strength of materials. However the resistance to be considered must take into consideration the history of the various layers at early age or due to shrinkage by means of eigenstresses. Finally, eigenstresses tend to vanish with time as a consequence of the decreasing shrinkage rate of the overlay and viscoelastic response of the materials. The time to decrease the maximum eigenstresses by a factor 2 is however counted in years rather than in month.

5.4 Different Forms of Restraint and Effect of Joints

Restraint can be defined as all mechanical effects that counteract the deformations of a given body.

At the micro level of heterogeneous materials such as concretes, the aggregates act as a restraint to the deformations of the cement paste under all kinds of shrinkage. The effect of this "internal restraint" on the onset of stresses and microcracks was numerically demonstrated among others by Sadouki [4]. The

same applies to Steel Fibre Reinforced Concretes, for which the fibres may significantly decrease the apparent shrinkage.

- The frictional forces on the subgrade of slabs on grade are another major source of restraint extensively studied in the literature. This effect is commonly described by interface models with adapted Mohr–Coulomb models.
- The flexural and axial stiffness of the substrate on which an overlay is applied
 act as a restraint. The combined axial and flexural stiffness of the composite
 system formed of substrate and overlay have to be considered to determine the
 degree of restraint of the overlay.
- The restraint by dowels is the main effect governing the structural behaviour of steel-concrete composite beams, as well as any other combination of different layers of different materials, linked by connectors.
- Reinforcement bars and in some cases formworks also act as a restraint to the deformations of cementitious materials at early age and long term, according to Bernard [3].
- Finally, the static system of a structural member also provides a restraint which acts on different degrees of freedom.

On the other hand, joints (artificial or cracks) in a composite structure act as a local release of the restraint, with varying consequences on the overall behaviour, positive or negative. The combination of the various kinds of restraint and of the joints defines the *kinematic system*.

5.5 Mechanical Behaviour of Composite Structures with Cementitious Materials of Different Ages

5.5.1 Overview of Existing Analytical Models

In what follows, the focus will be put on the description of the mechanical response of composite structural members under differential shrinkage. The existing analytical models can be classified on the basis of three main features:

- consideration of the flexural degree of freedom (effect of curvature);
- consideration of partial debonding;
- consideration of the viscoelastic behaviour of overlay and substrate.

There are two major internationally accepted analytical theories for the modelling of bonded concrete overlays. These are the theories presented by Birkeland [5], which does not consider debonding, and the one from Silfwerbrand [1, 6] which does. The models presented by Alonso-Junghanns [7], Silfwerbrand [1, 2], Bernard [3], Denarié et al. [8], and Hartl [9, 10] are essentially adaptations and modifications of Birkeland's theory. The prestress analogy (introduction of concentrated forces at the free ends of a composite member to model the effect of shrinkage) which is applied

in the models based on Birkeland's theory, is convenient to use, especially because it is easy to understand and easy to apply.

Beushausen [11] questioned both: (1) existing analytical models based on the prestress analogy, in their way to describe the introduction of forces in a composite member subjected to differential shrinkage of an overlay, and (2) the use of the Bernoulli principle in the derivation of most models. This author presented a semi-empirical analytical model for the analysis of restrained overlay shrinkage stresses based on localised, i.e. non-linear strain and stress conditions inside the composite member. Extensive strain measurements were realized on composite specimens with various geometries and aspect ratios (curvature free or prevented), with different surface preparations of the substrate. As expected, for deep composite elements with aspect ratio l/h < 1, Bernoulli's principle of plane sections remaining plane after being stressed does not apply [12–14].

On a general basis, one must keep in mind that shrinkage of an overlay corresponds to an imposed displacement, not an imposed force or imposed distributed forces. It is clear that the displacement due to shrinkage is partly restrained on all the length of the interface with the substrate. This however does not imply that the resulting reaction of the substrate leads to constant shear forces along the interface. At the contrary, for "slender geometries" with l/h superior to 5, following what was shown by Jonasson [15] and Haardt [16], a simple finite element simulation of a drying overlay on a substrate leads to concentrated shear forces in the interface, at the extremities of the member, similar to the predictions of the "prestress analogy", which turns out to be well adapted to simply represent a composite member with shrinkage of the overlay.

In what follows, the two main approaches will be referred to as:

- *Perfect bond* by Silfwerbrand [1, 2], further generalized by Bernard [3] and modified by Denarié et al. [8].
- Partial debonding, from Silfwerbrand [1, 17].

5.5.2 Normal Stresses Due to Differential Shrinkage in Composite Beams with Complete Bond

Stresses due to restrained movements can principally be computed by the product of three factors according to the following equation:

Stress = stiffness \times free strain \times degree of restraint

Consequently, all three factors are equally important. The stiffness is dependent on modulus of elasticity but also on creep or relaxation. The free strain is the strain that a completely free member would develop due to thermal or moisture changes, shrinkage, or any other internal or external source causing volumetric change of the member material. The degree of restraint μ defines the conditions of restraint as the ratio between the actual stress σ_{rest} taking into consideration the effective stiffness

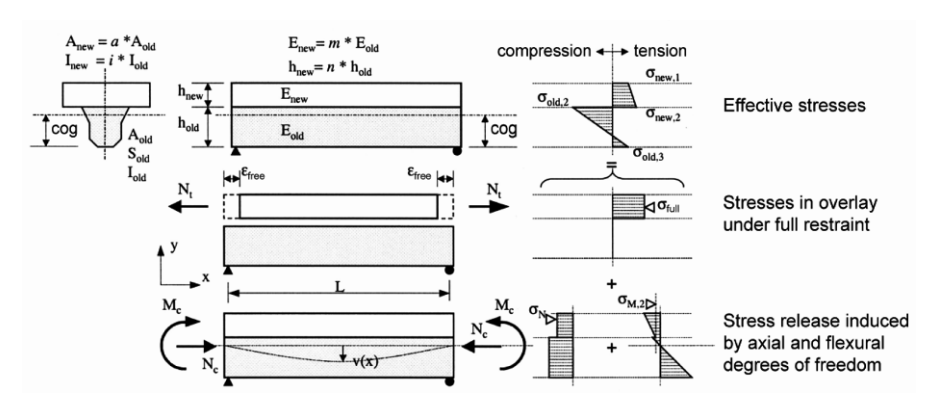


Fig. 5.2 Eigenstresses in a statically determinate composite member, combination of axial (σ_N) and flexural $(\sigma_{M,2})$ release effects (adapted from [3])

of the composite structure and the stress σ_{full} that would occur in a totally restrained composite structure:

$$\mu = \frac{\sigma_{\text{rest}}}{\sigma_{\text{full}}} \tag{5.1}$$

Restraints can be associated to all degrees of freedom of a structure. For a composite beam, two degrees of freedom can be realized, one axial, one flexural. Many structural engineers are not aware of the fact that complete bond between overlay and substrate does not necessarily cause complete restraint in the repaired concrete structure. The reason is that the stiffness of the remaining part of the old structure is not infinite. The striving of the overlay to contract is only partly prevented by the remaining part of the old structure. The absence of a complete restraint leads to substantial stress reductions. Combined with creep these reductions will limit the maximum tensile stress below the tensile strength and, hence, explain the absence of shrinkage cracking. The easiest way to explain this is by studying a composite beam exposed to differential shrinkage. This analysis was done first by Silfwerbrand [1] for rectangular layers of equal width, and generalized by Bernard [3] to distinguish the contribution of the various degrees of freedom, for arbitrary cross sections of the two layers, as shown in Figure 5.2, for a statically determinate beam, with $\sigma_{\text{new, 2}}$ [MPa]: tensile stress in the new layer at the interface, μ : degree of restraint, $\varepsilon_{\text{free}}$: mean shrinkage strain in the new layer, cog: centre of gravity of the composite section, h_{new} , cog_{new} , A_{new} , S_{new} , I_{new} , resp. height, centre of gravity, area, static moment and inertia of the new section (overlay), $h_{\rm old}$, $cog_{\rm old}$, $A_{\rm old}$, $S_{\rm old}$, $I_{\rm old}$, resp. height, centre of gravity, area, static moment and inertia of the old section (substrate), and $n = h_{\text{new}}/h_{\text{old}}$, $m = E_{\text{new}}/E_{\text{old}}$, $a = A_{\text{new}}/A_{\text{old}}$, $i = I_{\text{new}}/I_{\text{old}}$, I_{comp} = inertia of the composite section.

The degree of restraint is calculated under the following hypotheses: linearelastic material behaviour, Poisson's ratio $\nu=0$, cross-section of the new layer is a rectangle, the cross-section of the substrate can be of any shape, and plane sections remain plain (hypothesis of Bernoulli), perfect bond between new layer and

substrate. As a consequence, the calculations only apply for the case of slender composite beams (l/h < 5). For deep elements such as walls on slabs, with l/h < 5, similar principles can be applied. The calculation of the strains and stresses has however to be adapted.

The principle of the analysis (prestress analogy) consists in determining the tensile force N_t that is necessary to compensate the free shrinkage deformation $\varepsilon_{\rm free}$ in the new layer. The tensile force is balanced in the composite member by a compressive force N_c and a bending moment M_c acting at the centre of gravity (cog) of the composite section. The stress state in the composite element is determined by the superposition of the resulting effects of N_t , N_c and M_c on the composite cross section. The resulting stress is the sum of the stress in the case of a total restraint, corresponding to the effort N_t , plus the relaxing effects due to the axial (N_c – stress σ_N) and flexural (M_c – stress $\sigma_{M,2}$) degrees of freedom. The axial release effect inducing the stress σ_N is constant throughout the overlay thickness. This is not the case of the flexural release effect inducing the stress σ_M which is maximum at the top of the overlay and has its smallest value in the overlay nearby the interface. In order to estimate the maximum overall stress in the overlay, the flexural release effect is evaluated at its location of minimal value, i.e., nearby the interface, and is noted $\sigma_{M,2}$.

In his original analysis, Bernard [3] proposed to define the degree of restraint as the sum of "1" plus the axial factor μ_N plus the flexural factor μ_M : both factors are negative in their individual expressions.

In the following, this approach is slightly modified, to define the degree of restraint as "1" minus the axial release minus the flexural release (Equation (5.2)), to associate the notion of degree of restraint to the effect of release of the stresses for each degree of freedom available, in a more straightforward way [8].

$$\mu = \frac{\sigma_{\text{new},2}}{\sigma_{\text{full}}} = \frac{\sigma_{\text{full}} + \sigma_N + \sigma_{M,2}}{\sigma_{\text{full}}} = 1 - \mu_N - \mu_M \tag{5.2}$$

The individual expressions of the release factors are adapted from [3]:

$$\mu_N = \frac{-\sigma_N}{\sigma_{\text{full}}} = \frac{ma}{ma+1} = \frac{1}{1+1/ma} = \frac{1}{1+\frac{E_{\text{old}} \cdot A_{\text{old}}}{E_{\text{max}} \cdot A_{\text{min}}}}$$
(5.3)

$$\mu_{M} = \frac{-\sigma_{M,2}}{\sigma_{\text{full}}} = \frac{N_{t}(\cos_{\text{new}} - \cos)}{W_{2}} \frac{1}{E_{\text{new}} \cdot \varepsilon_{\text{free}}}$$

$$= \frac{A_{\text{new}} \cdot (\cos_{\text{new}} - \cos) \cdot [m \cdot (h_{\text{old}} - \cos)]}{[I_{\text{old}} + A_{\text{old}}(\cos - \cos_{\text{old}})^{2} + m \cdot (I_{\text{new}} + A_{\text{new}}(\cos_{\text{new}} - \cos)^{2})]}$$
(5.4)

With W_2 : resisting moment of the composite section, at the level of the interface, I_{comp} : inertia of the composite section, y_2 , lever arm between cog and interface (location of stress $\sigma_{\text{new},2}$)

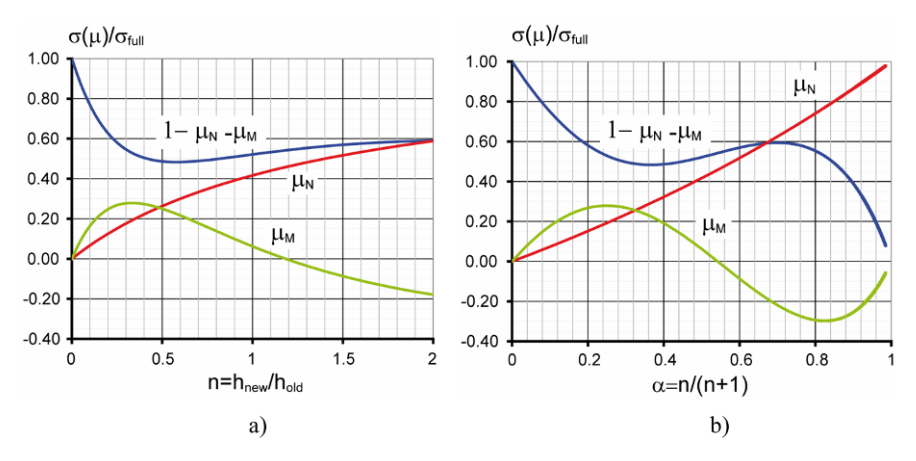


Fig. 5.3 Axial and flexural effects on restraint as a function of (a) $n = h_{\text{new}}/h_{\text{old}}$ and (b) $\alpha = h_{\text{new}}/(h_{\text{old}} + h_{\text{new}})$, with m = 0.71 and $h_{\text{old}} = h_{\text{new}}$, after [8]

$$cog = \frac{S_{old} + m \cdot S_{new}}{A_{old} + m \cdot A_{new}}$$
 (5.5)

$$W_2 = \frac{I_{\text{comp}}}{y_2}$$

$$= \frac{[I_{\text{old}} + A_{\text{old}}]}{(\cos - \cos_{\text{old}})^2 + m \cdot (I_{\text{new}} + A_{\text{new}}(\cos_{\text{new}} - \cos)^2)]} m \cdot (h_{\text{old}} - \cos)$$
(5.6)

It is worth mentioning that the release factor μ_N associated to the axial degree of freedom corresponds to the approach proposed by Alonso Junghans [7].

The graphical representation of equations (5.2) to (5.6) is shown in Figure 5.3 for m=0.71 ($E_{\rm new}=25$ GPa and $E_{\rm old}=35$ GPa) and rectangular sections of similar width for the old and new layers ($h_{\rm old}=h_{\rm new}$). The axial release μ_N increases in a monotonic way when the thickness of the new layer increases. The flexural release μ_M first increases, reaches a maximum and then decreases down to 0 when the centre of gravity (COG) of the composite cross section enters the new layer, to become then negative. Two representations are shown: (a) with the ratio of the layer thicknesses n, and (b) with the ratio α between the thickness of the new layer and the total thickness of the composite section as x-axis.

The range of most cases encountered in practice corresponds to the domain shown in Figure 5.3a with parameter n on the x-axis. For the chosen set of parameters, the global restraint varies in a significant way for values of n smaller than 0.3. For values of n larger than 0.3, the overall degree of restraint is almost constant and equal to 0.5 to 0.6.

Silfwerbrand [1, 2] generalized this method for various combinations of materials, as shown in Figure 5.4a, and to different boundary conditions [17]. When the

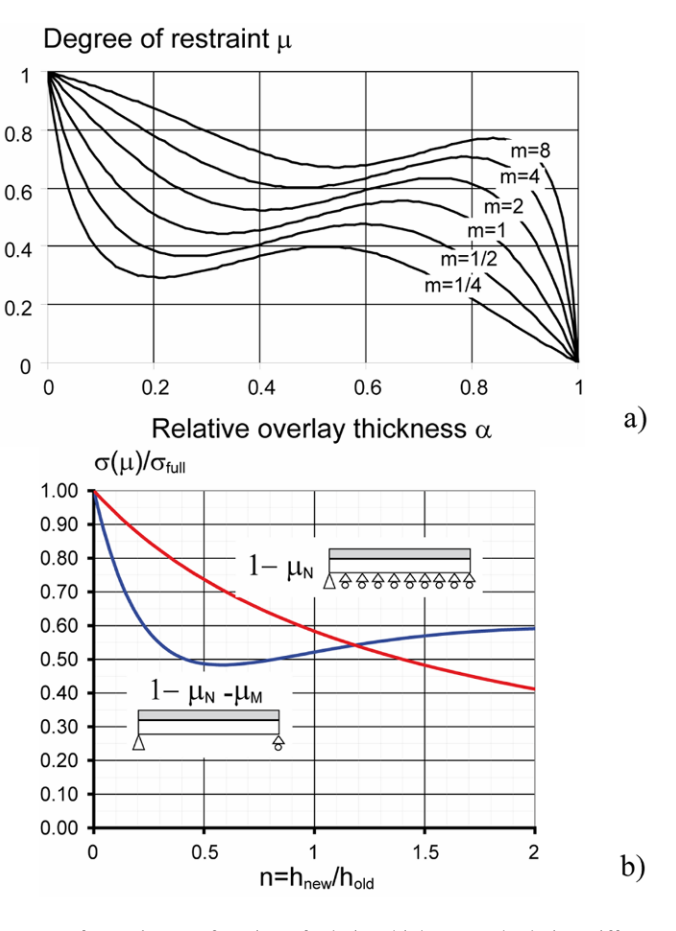


Fig. 5.4 (a) Degree of restraint as a function of relative thickness and relative stiffness, after [1, 2]. (b) Effect of statical boundary conditions with m = 0.71 and $h_{\rm old} = h_{\rm new}$

flexural degree of freedom is almost or fully blocked (for example in the middle spans of hyper static multiple span beams), only axial release acts and the degree of restraint is given by $\mu = 1 - \mu_N$, as illustrated in Figure 5.4b.

Concrete viscoelasticity has a beneficial effect on the developed stresses due to differential shrinkage, in terms of relaxation. An engineering approach to estimate this effect is to replace the modulus of elasticity $E_{\rm new}$ of the overlay with a fictitious modulus of elasticity $E_{\rm new}^* = E_{\rm new}/(1+\phi_{\rm new})$ and $E_{\rm old}$ with $E_{\rm old}^* = E_{\rm old}/(1+\phi_{\rm old})$, where $\phi_{\rm new}$ and $\phi_{\rm old}$ are the creep coefficients of the overlay and base concrete, respectively. The maximum tensile stress in the overlay may be computed by the following equation according to Silfwerbrand [2, 18]:

$$\sigma_{\text{max}} = \frac{m^*(1-\alpha)(m^*(1-\alpha)^3 + \alpha^2(3+\alpha))}{m^* + (m^*-1)(m^*(1-\alpha)^4 - \alpha^4)} \cdot \frac{E_{\text{new}}}{1+\varphi_{\text{new}}} \cdot \varepsilon_{\text{free}} = \mu \cdot \frac{E_{\text{new}}}{1+\varphi_{\text{new}}} \cdot \varepsilon_{\text{free}}$$
(5.7)

with

$$m^* = \frac{E_{\text{old}}^*}{E_{\text{new}}^*} = \frac{E_{\text{old}}/(1 + \varphi_{\text{old}})}{E_{\text{new}}/(1 + \varphi_{\text{new}})} = \frac{E_{\text{old}}}{E_{\text{new}}} \cdot \frac{1 + \varphi_{\text{new}}}{1 + \varphi_{\text{old}}} \approx 1 + \varphi_{\text{new}}$$

since $E_{\text{new}} \approx E_{\text{old}}$ and $\phi_{\text{old}} \approx 0$.

Since the development of drying shrinkage starts as soon as the curing of the new-cast overlay is ended, also the stresses due to differential shrinkage start to develop at an early stage. This means that also the creep starts at an early stage, before the concrete is mature. This will in turn lead to a large amount of creep. Creep coefficients of 5 to 6 have been measured [2, 18]. The beneficial influence of creep is shown in the following example of computation of stresses due to differential shrinkage in a repaired concrete beam.

Geometrical and material data: $\alpha=2/7~(\approx 0.286),~E_{\rm new}=E_{\rm old}=35~{\rm GPa},~\varepsilon_{\rm free}=0.45~{\rm mm/m}.$

Case (a) Full restraint $\mu = 1 \rightarrow \sigma_{\text{full}} = E_{\text{new}} \cdot \varepsilon_{\text{free}} = 15.8 \text{ MPa}.$

Case (b) Beam theory with neglected creep $\rightarrow m=1, \mu=0.452$ and $\sigma_{\rm full}=7.12$ MPa.

Case (c) Beam theory with creep coefficients $\phi_1=4$ and $\phi_2=0 \rightarrow m=0.2$, $\mu=0.733$, and $\sigma_{\rm full}=2.31$ MPa.

The maximum normal stress diminishes from 16 to 2.3 MPa. The latter value is of the same magnitude as the tensile strength of concrete. It explains why some overlays are crack-free while cracks are visible in others. The creep factors assumed in this example are theoretical estimates to illustrate the possible effect of relaxation of stresses due to viscoelastic effects.

One must however also mention that the resistance of cementitious materials subjected to long term tensile actions with low loading rates such as shrinkage is significantly lower than the resistance obtained from quasi static tensile tests. This effect has to be considered when evaluating the risk of cracking at early age or long term in bonded overlays.

Beushausen et al. [19] estimated the relaxation in overlays from experimental tests on composite concrete/concrete members. Strain measurements on free and restrained materials and time of cracking were used to determine the relaxation at a given time. Values of 40 to 50% were found. More generally speaking, these authors propose an incremental method to determine the relaxation factor as a function of time.

A more precise analytical approach of the effect of linear viscoleasticity on the relaxation of stresses in composite members can be found in the multilayer theory from Huet [20], adapted from the elastic case from Siestrunck et al. [21].

Finally, the viscoelastic response depends on the stress level above certain limits. There is no general agreement in the literature on the threshold value above which viscoelastic response would be significantly influenced by the stress level. Gustch et al. [22] and Horimoto et al. [23] tend to show that the relaxation under tension is not significantly influenced by the stress level. Denarié et al. [24] showed that relaxation starts to deviate from a linear response at load levels around 50% in Wedge Splitting Tests. However, for this specific testing geometry with a strong strain gradient, the material enters the softening domain at the notch tip for load levels close to 50%. At this level, the deviation from non-linearity corresponds to the beginning of activation of the tensile strain softening (equivalent load level 100% under uniaxial tension).

Under creep, it is well known that deviation from a linear viscoelastic response start to be clear above 40 to 50% under compression and tension.

On the other hand, for high degrees of restraint, stresses can very quickly be in the range of the quasi-static tensile strength. At those levels of loading, linear viscoelastic models do not apply anymore and any substantial increase in the viscoelastic response is likely to be due to ongoing damage.

Reliable relaxation tests under tension, at various load levels pre peak are extremely difficult to perform and constitute an interesting and necessary challenge for future research.

5.5.3 Shear Stresses Due to Differential Shrinkage in Composite Beams

The simple beam model (described in Section 5.5.2) assuming complete bond between overlay and base (substrate) is easy to use and gives decent estimations of normal stresses in the interior parts of overlay and base. However, in reality horizontal cracking leading to debonding sometimes is observed especially in vicinity to the vertical borders and joints of the repaired structure. In order to estimate the probability for debonding or explain its presence if it already exists, we need to be able to estimate shear stresses along the interface between overlay and substrate. Jonasson [15] has developed a simple model that also has been used by FIP [25]. Jonasson made computer investigations and found that the shear stress has its maximum magnitude at the boundary of the structure and diminishes approximately linearly to zero at a distance approximately equal to three times the thickness of the overlay (Figure 5.5).

By utilizing the symbols presented above, the maximum shear stress τ_{max} is given by the following equilibrium equation:

$$\tau_{\text{max}} = \frac{2}{3} \cdot \frac{F}{b\alpha h} \tag{5.8}$$

where αh and b are the thickness and width of the overlay, respectively, and F is the resultant to the normal stresses in the overlay, i.e.

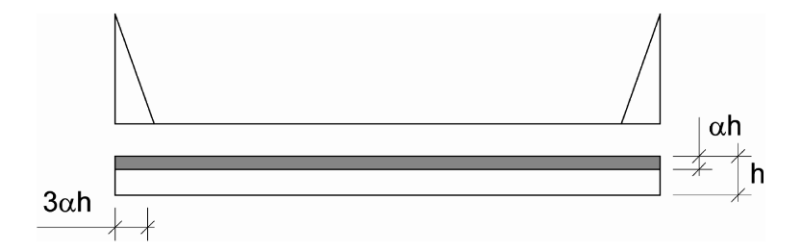


Fig. 5.5 Shear stress distribution according to [15]

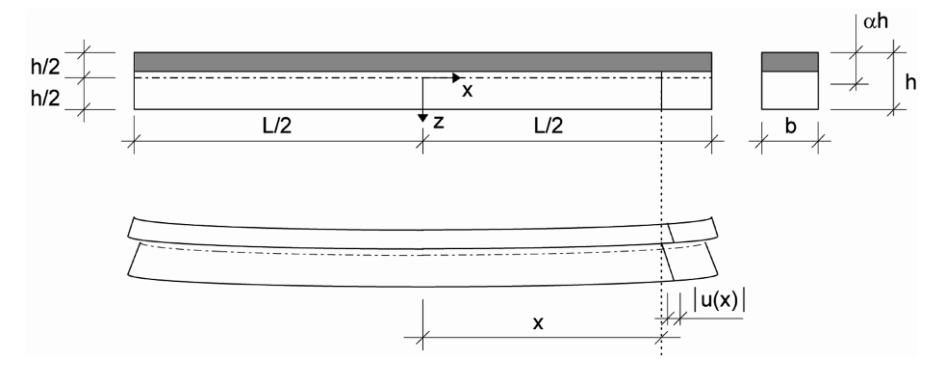


Fig. 5.6 Composite beam with incomplete bond between overlay and base (substrate) [1, 6]

$$F = \int_{\alpha h} \sigma(z) \cdot b \cdot dz \tag{5.9}$$

For the simply supported or free composite beam (Figure 5.3), the maximum shear stress could be computed by the following equation (if creep is considered):

$$\tau_{\text{max}} = \frac{2}{3} \cdot \frac{m(1 - 4\alpha + 6\alpha^2 - 3\alpha^3 + (m - 1)(1 - \alpha)^4)}{m + (m - 1)(m(1 - \alpha)^4 - \alpha^4)} \cdot \frac{E_1}{1 + \phi_1} \varepsilon_{cs}$$
 (5.10)

5.5.4 Normal and Shear Stresses Due to Differential Shrinkage in Composite Beams with Incomplete Bond

A shortcoming with the simple beam model described in Section 5.3 is that it leads to constant normal stresses along the beam in cases with symmetrical boundary conditions. Since the shear stress is the derivative of the normal stress with respect to the length coordinate, constant normal stresses result in zero shear stresses. In reality, shear stresses appear in the vicinity to vertical boundaries, vertical joints, and vertical cracks, if any.

Silfwerbrand [1, 6] has developed an engineering beam model considering incomplete bond between overlay and base. By using this model, it is possible not only to compute normal stresses and strains along the beam, but also shear stresses $\tau(x)$ and horizontal slip u(x) along the interface. This model uses a linear relationship between shear stress and horizontal slip between overlay and base, i.e., $\tau(x) = K \cdot u(x)$, where K is a constant of proportionality.

The shear stresses can be computed by the following equation [6]:

$$\tau(x) = -\frac{m\alpha(1-\alpha)(1-3\alpha(1-\alpha)+(m-1)(1-\alpha)^3)}{m+(m-1)(m(1-\alpha)^4-\alpha^4)}$$

$$\cdot \frac{E_1}{1+\phi_1} \cdot \varepsilon_{cs} \cdot \frac{h}{L} \cdot \lambda L \cdot \frac{\sinh \lambda x}{\cosh \lambda L/2}$$
(5.11)

$$(\lambda L)^{2} = -\frac{m + (m-1)(m(1-\alpha)^{4} - \alpha^{4})}{m\alpha(1-\alpha)(1-3\alpha(1-\alpha) + (m-1)(1-\alpha)^{3})} \cdot \frac{1+\phi_{1}}{E_{1}} \cdot \frac{KL^{2}}{h}$$
(5.12)

The engineering problem is to estimate the coefficient K and, hence, the governing non-dimensional product λL . Direct tests are difficult since the horizontal slip u is difficult to measure and likely to be dependent on loading rate. The interesting rate is given by the shrinkage velocity and such slow tests are if not practically impossible at least economically impossible. However, the effect of varying values of the product λL could easily be studied (Figure 5.7), with $z^* = z$ coordinate at interface.

Shear stresses increase with increasing λL value and normal stresses approach the constant distribution given by the simple beam model with complete bond (Section 5.3).

Normal stresses can be seen as the reflection of the strains and vice versa. The normal stress vanishes at the beam edges and has its maximum value in the interior parts of the beam. The strain (that contrary to stress is easy to measure) has, consequently, its maximum variation at the edges. This relationship has been verified by strain measurements in two 6 and 8 m long repaired concrete beams subjected to 14 months of differential shrinkage [1]. By considering creep effects and comparing the measuring results with computed strain curves for varying λL values, it was concluded that $\lambda L = 54$ gave the best fit to the 8 m long beam (Figure 5.8). This value has in turn been used to estimate the shear stresses in this beam (Figure 5.9).

The maximum shear stress is estimated to 1.6 MPa, i.e., probably below the shear strength of concrete. This computation result is an explanation to the fact that no cracks were observed in the test beams [1].

The computation result also shows that the simple shear stress computation model [15] described in Section 5.3 gives a fairly good estimation of both maximum shear value and its corresponding triangular shape.

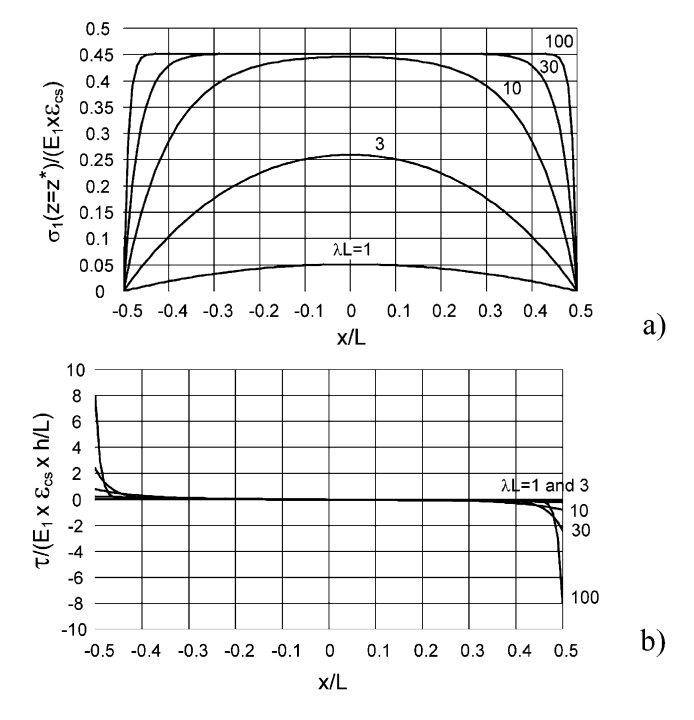


Fig. 5.7 (a) Maximum relative normal stresses (= ψ) and (b) relative shear stresses along a simply supported composite beam due to differential shrinkage. $m=1, \alpha=2/7, \phi_1=\phi_2=0$, after [1, 6]

5.6 Experimental Tests

Various authors have performed tests on composite structural members. However, very few have produced results that support or discard models.

5.6.1 Swedish Tests on Mechanically Loaded Concrete Beams

Silfwerbrand [26] carried out tests on simply supported composite concrete beams subjected to a static load at mid span (Figure 5.10). The substrate concrete was sawn from a 70 year old bridge (Skurubron). It had a compressive strength of 85 MPa (measured on drilled cores). The substrate concrete was chipped with pneumatic hammers prior to overlay casting. The measured compressive cube strength of the overlay was 60 MPa. For comparison, additional test beams made of new-cast concrete were included in the investigation. Bonding agents were used in two cases. The beams were tested upside down producing tension in the overlay. As shown in Table 5.1, the composite beams with hammered interfaces developed equally high

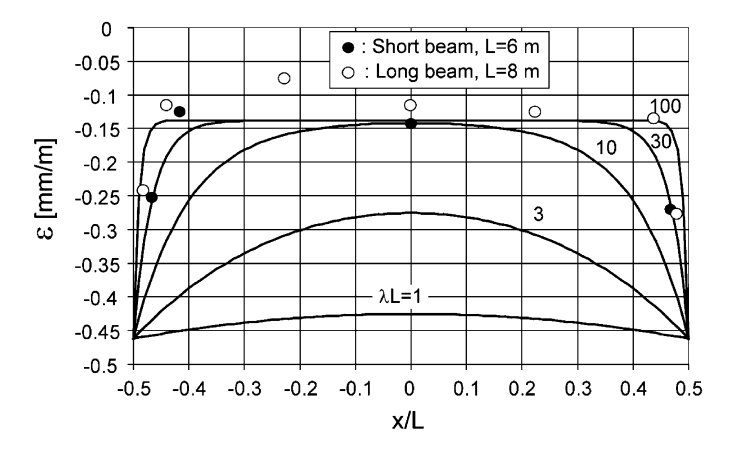


Fig. 5.8 Measured strain values and computed ones, from [6]

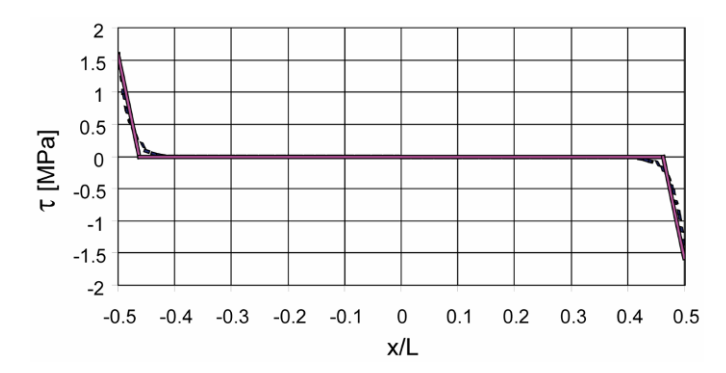


Fig. 5.9 Computed shear stresses for an example based on geometrical and material data for the 8 m long beam [6, 18]. Solid line = simple model proposed by Jonasson [15], dotted line = model for incomplete bond [6]

failure loads and obtained same failure mode as the homogeneous beam. Obviously, the bond between substrate and overlay was sufficient. On the contrary, a smooth, steel grinded interface does not provide sufficient bond to promote composite action. In both beams with this interface, a premature interface failure occurred. After the interface failure, the (reinforced) bottom part of the beam was able to carry an increasing load, but not to the same level as the other beams.

| Interface | | | Static tests | |
|--------------------|-------------------|------------------------|-------------------|-------------------|
| Preparation | Bonding agent | Other treatment | Failure load (kN) | Failure mode |
| Pneumatic hammer | No | | 130 | Shear |
| Pneumatic hammer | Epoxy adhesive | | 150 | Shear |
| Pneumatic hammer | No | Vacuum treated overlay | 130 | Shear |
| None (homogeneous) | No | | 130 | Shear |
| Steel grinded | No | | 40 & 70* | Interface & Shear |
| Steel grinded | Mortar | | 17 & 69* | Interface & Shear |

Table 5.1 Tests on mechanically loaded concrete beams [26]

^{*} The composite beam first cracked at the interface; subsequently, the load could be increased markedly to shear failure in the bottom (reinforced) part of the beam.

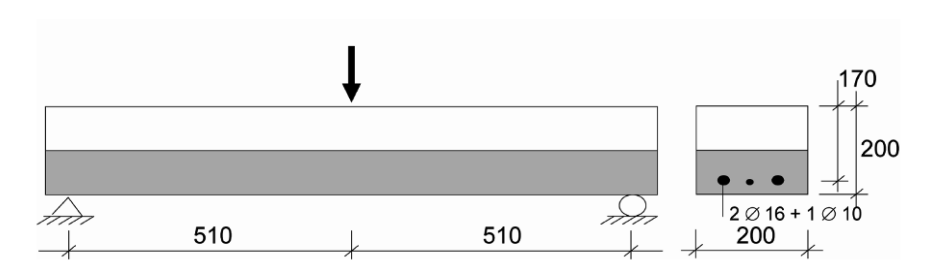


Fig. 5.10 Test specimen and loading case in beam tests (unit: mm) [26]

5.6.2 Swedish Tests on Concrete Beams Subjected to Differential Shrinkage

Differential shrinkage is considered to be an important loading case for concrete overlays. In order to study strain development and cracking, if any, four composite beams of varying length were cast and stored outdoors in a tent for 14 months [1]. The thickness ratio between overlay and total beam height was in all cases 2/7. Two beams were supported on soft airbags providing free curvature whereas the other two were supported on three solid supports preventing curvature (Figure 5.11). Old concrete columns constituted the substrate concrete. Drilled cores obtained a compressive strength of 62 MPa. The substrate concrete was chipped with pneumatic hammers prior to overlay casting. The surface was prewetted during a couple of days but superficially dry at overlay placement. No bonding agents were used. At the end of the tests, the concrete used for the overlays obtained compressive cube strength of 65 MPa. Maximum free shrinkage (measured on $400 \times 100 \times 100$ mm standard prisms) was 0.45 mm/m. Despite the magnitude of the free shrinkage and the bond providing restraint, no cracks were observed, neither in the overlays perpendicular to the beam length nor in the interface. Strain measurements supported

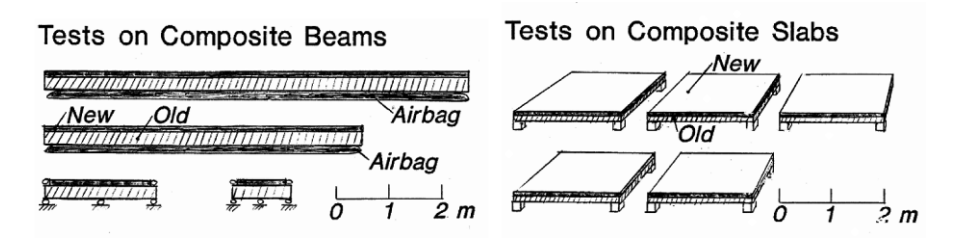


Fig. 5.11 Tests on composite beams [1] and composite slabs [18] subjected to differential shrinkage

composite action. After terminated tests, a bond strength averaging 1.9 MPa was obtained through pull-off tests.

5.6.3 Swedish Tests on Concrete Slabs

In mid 1980s, the water-jet technique was introduced in Sweden. In order to compare it with other methods of concrete removal and substrate preparation, slab tests were carried out at KTH in Stockholm, Sweden [18]. The preparation methods investigated included water-jet technique, pneumatic hammers, and sandblasting. The substrate surface was prewetted during three days but superficially dry at overlay placement. No bonding agent was used. The tests consisted of five composite slabs (Figure 5.12) and two homogeneous ones. The ratio between overlay thickness and total height was 1/3. The substrate concrete was seven months old at time of overlay placement. Differential shrinkage was investigated during six months under indoor conditions. No visible cracking occurred. Displacement measurements supported composite behaviour. At terminated tests, the compressive cube strength exceeded 50 MPa for both substrate and overlay concrete. The free shrinkage (measured on $400 \times 100 \times 100$ -mm prisms) of the overlay concrete was 0.6 mm/m. Simultaneously, the shrinkage of the old concrete increased with less than 0.05 mm/m.

In a second phase of the tests (Figure 5.12a), the five composite and the two homogeneous slabs were simply supported at the four corners and loaded to failure with a centrically placed static load.

The base layer was reinforced with 13 Ø 8 mm, s = 150 mm in both directions. The obtained load-displacement curves show a similar behaviour for all slabs. All slabs (including homogeneous ones) obtained approximately equally high ultimate loads between 83 and 98 kN (Figure 5.12b). Finally, the bond strength was investigated by pull-off tests (see Section 4.4).

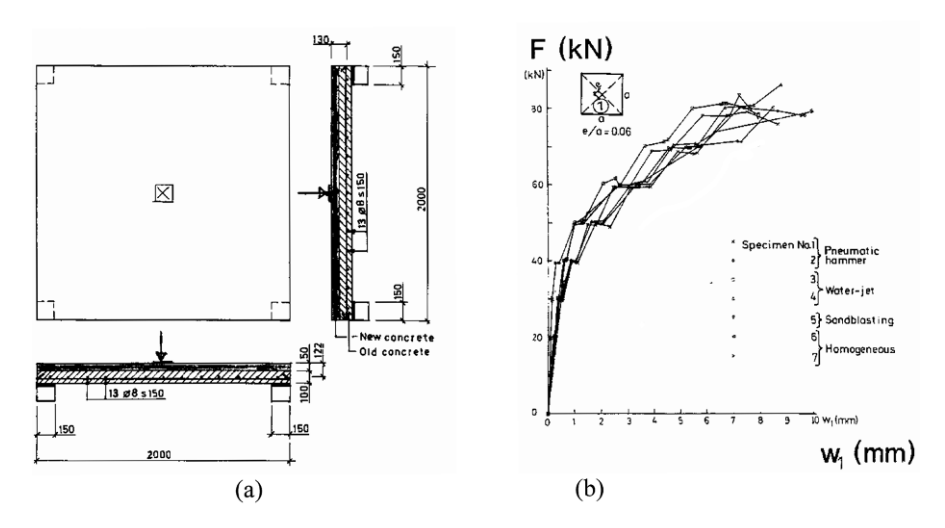


Fig. 5.12 Composite slab loading experiments: (a) experimental layout; (b) load-displacement curves [18]

5.6.4 Tests at EPFL on Composite Beams with Normal Concretes of Different Ages

Bernard [3] tested 14 composite beams with substrate dimensions length/width/ thickness of 5400/500/170 mm, hydrojetted with removal of 20 mm of concrete, and new concrete layers between 70 to 170 mm, with various reinforcement ratios, with reinforcement bars or steel fibres. The beams, placed in a controlled environment (20°C, 30% RH) were instrumented with external LVDT's and thermocouples and optical deformation sensors embedded in the substrate and the new layer. The substrates were between 70 and 237 days old when the overlays were cast. The new concretes composition was 300 kg/m³ CEM I 52.5 R, W/C = 0.50 without steel fibres and 350 kg/m³ CEM I 52.5 R and W/C = 0.5, with 80 kg/m³ steel fibres. The deformational behaviour of the composite members was monitored at early age for 3 to 6 days, and at longer term, up to 270 days, under creep loading. The optical deformation sensors measured total displacements in the central part of the beam (distance 2000 mm). The thermocouples gave the temperature at the same level. The measurements were started when the new concrete was cast and stopped after 100 hours. The main results from this study can be summarized as follows:

- the time lag between the end of chemical swelling and the peak of temperature
 in the upper part of the new layer and the evolution of strains are well predicted
 only if the autogenous shrinkage is taken into account in the numerical modelling:
- the autogenous shrinkage is the main phenomenon which induces curvature and tensile stresses at early age in the new layer of tested hybrid elements;

 in the conditions of these tests, the long term residual stresses due to autogenous shrinkage attain approximately 50 % of the maximum tensile stress at early age;

• the reinforcement in the new layer induces a significant restraint of the overall deformations of the composite member; for high reinforcement ratios of the new layer, this restraint can lead to cracking.

5.6.5 Other Tests

Finally, it is also worth mentioning the works by Chausson [27] that used a steel substrate with a grinded surface to simulate a concrete substrate. This method has significant advantages in terms of reutilization of the substrates for several tests.

5.7 On Restrained Shrinkage Set-ups

Another way to experimentally investigate the effect of restraint on the development of stresses and the risk of cracking, without having to test costly large size structural members, is given by so called "restrained shrinkage testing devices". These devices have been known for many years now, starting with so-called "cracking frames" [28], where the restraint is passive. Active systems were proposed by Kovler [29]. Finally, so called *Temperature-Stress Testing Machines* – TSTM are systems with active restraint by means of closed-loop-testing machines as well as cooling circuits placed around the specimens, to impose temperature conditions at will [30–36].

Such systems can be used either in isothermal conditions to isolate fundamental material properties such as autogenous shrinkage, or to test overlay materials in realistic conditions of restraint and curing, thus providing and "experimental simulation tool".

In a similar way, to induce a high restraint with compact dimensions, Martinola [37] used instrumented ring geometry, inspired from the "Bolomey" ring shrinkage test.

5.8 Numerical Modelling

The numerical modelling of the structural behaviour of bonded concrete overlays and more generally of composite concrete-concrete structural members has been realized in various ways in the past, with either general purpose finite element packages, specifically oriented packages for multi-layer systems, or original numerical solutions of mathematical formulations of the problem. Basically, any finite element

package is able to model multi layer systems. The main differences come from the ability of the software to deal with more advanced material properties such as:

- time-dependent evolution of the mechanical properties of the overlay and substrate – maturation;
- comprehensive simulation of the physical processes such as drying, release of heat of hydration, thermal transport;
- viscoelasticity and ageing;
- non-linear crack propagation (smeared crack models or discrete crack models);
- interface between two layers;
- · reinforcing bars.

It is impossible to quote all modelling works on hybrid systems however, among the most recent ones, one can mention the following:

Bernard [3, 38, 39] used the finite element package MLS (Multi-Layer Systems) from FEMMASSE [40], with a comprehensive description of thermo-hygromechanical processes in multi-layer systems, at early age and long term, including effects of maturation, viscoelasticity, reinforcement in the overlay and non-linear fracture mechanics (smeared crack model) for the bulk of the materials and for interfaces. The significant role of autogenous shrinkage at early age on the structural response of hybrid elements with concretes and the consequences of the restraining effect of reinforcement bars in the new layer were demonstrated. The results include an extensive parametric study on the effect of the overlay thickness and reinforcement ratio on the risk of delamination. Habel [41, 42] used the same package with material models extended to the case of tensile hardening fibre reinforced composites to model composite beams with Ultra-High Performance Fibre Reinforced Concrete (UHPFRC) overlays.

Martinola [37, 43] used FEM package DIANA [44] for thermo-hygro-mechanical calculations with a strong emphasis on moisture transport and self-desiccation, in order to study the risk of cracking and delamination of composite structural systems. Realistic interfacial constitutive laws were used with parameters from experimental tests. Based on comprehensive experimental tests, the hygro-mechanical coupling coefficient was implemented in the code as a function of the moisture content, and the major influence of this variation was demonstrated. A parametric study was performed and recommendations for the design of bonded concrete overlays were given.

Laurence [45] used software CESAR-LCPC to calculate the evolution of stresses at early age and long term in bonded concrete overlays. The modules TEXO, MEXO and HEXO of the finite element package were used to calculate the stresses induced by thermo-chemo-mechanical effects at early age, taking maturation into consideration, for linear elastic materials. In a second step, the effect of drying shrinkage, including water absorption by the substrate, was introduced. The results showed the very significant influence of autogenous shrinkage as well as of the absorption of water by the substrate on the development of stresses in the overlay.

Finite elements computations of composite structures with bonded overlays subjected to drying have been performed by Tran et al. [46] using the FEM code

CAST3M. They take into account the effects of the shrinkage and of the loads applied on an overlaid structure. Shrinkage is computed from the water loss associated, (1) to the hydration process, (2) to the water exchanges with the surrounding (mainly evaporation). The results faithfully represent the experimental relationship between measured shrinkage, applied loads and debonding. Apart from the boundaries, the Bernoulli principle appears as valid.

Féron [47] developed a mechanical model to determine the stresses in multilayer systems due to shrinkage, taking into consideration ground friction and chemothermo-hygro mechanical couplings in the materials. The water loss was calculated from diffusion laws by finite differences. The calculation of deformations and stresses in the multilayer system relies on the assumptions of (1) a perfectly bond between the layers, and (2) the respect of the Navier–Bernoulli principle. This model has been validated by comparative finite element simulations and successfully applied to the cases of industrial floors with Fibre Reinforced Concretes and repair layers.

HIPERPAV [48–51], although not a finite element code, takes into consideration thermo-hygro-mechanical phenomena by means of semi-empirical mathematical formulas from codes or recommendations, to predict the risk of cracking in overlays. The physical processes involved (thermal and moisture transport) are based on semi-empirical analytical solutions for current geometries.

The model from Rostasy et al. [52] is also numerical-analytical but includes very comprehensive descriptions of the physical and mechanical phenomena acting at early age and long term in composite structures. Although more dedicated to massive structures, walls on slabs for instance, this model is also applicable to overlays on substrates.

5.9 Conclusions

- Composite structural members are very common. They are however still often designed on an empirical basis.
- The notion of degree of restraint, associated to the degrees of freedom of a
 composite structural member provides a common background for the analysis
 of various practical applications among which are cement based overlays on
 existing concrete substrates, under restrained shrinkage.
- This notion initially derived for linear elastic overlay materials case can be extended to viscoelastic materials.
- This approach enables one to predict in a realistic way the stresses induced by restrained deformations and access the risks of cracking in the new layers.
- It can be further extended to three dimensional structures such as slabs, or to
 include the restraining effect of reinforcement bars in the substrate or in the
 new layer.

• For current cases of application (overlays on flexible substrates), in the linearelastic case, the degree of restraint varies between 0.4 and 0.8 and can be calculated from simple geometrical and material parameters.

• Shear stresses at the interface of composite members can be accurately predicted, taking into consideration partial debonding.

5.10 Outlook for Future Research

- Experimental tests to determine accurately the strain profiles/distributions in various cases of member slenderness and combinations of materials.
- Extension to 3D (case of slabs) of analytical models taking into consideration the degree of restraint.
- Determination of design values of the time/rate dependent tensile strength.
- Implementation of non-linear viscoelastic models adapted for calculations with high stresses high degrees of restraint.
- Relaxation tests under tensile loading at various pre-peak load levels, with temperature control of the specimen.

References

- Silfwerbrand, J., Differential shrinkage in composite concrete beams of old concrete and a new-cast concrete overlay. Bulletin No. 144, Department of Structural Mechanics and Engineering, Royal Institute of Technology, Stockholm, Sweden, 149 pp., 1986 [in Swedish].
- Silfwerbrand, J., Differential shrinkage in normal and high strength concrete overlays. Nordic Concrete Research, 19, 55–68, 1996.
- 3. Bernard, O., Comportement à long terme des éléments de structure formés de bétons d'âges différents. Doctoral Thesis, Swiss Federal Institute of Technology No. 228, Lausanne, Switzerland, 2000. (in French).
- Sadouki, H., Simulation et analyse numérique du comportement mécanique de structures composites, Doctoral Thesis, Swiss Federal Institute of Technology No. 676, Lausanne, Switzerland, 1987 [in French].
- Birkeland H.W., Differential shrinkage in composite beams. *Journal of the American Concrete Institute*, 1123–1136, May 1960.
- 6. Silfwerbrand, J., Stresses and strains in composite concrete beams subjected to differential shrinkage, *ACI Structural Journal*, **94**(4), 347–353, 1997.
- 7. Alonso Junghans, M.T., Zur Risssicherheit zementgebundener dehnungsbehinderter Schichten unter Berücksichtigung von Dauereinflüssen. Ph.D. Thesis, Universität Hamburg-Harburg, Shaker Verlag, Aachen, Germany, 1997 [in German].
- Denarié, E. and Silfwerbrand, J., Structural behaviour of bonded concrete overlays. In *Proceedings International RILEM Workshop on Bonded Concrete Overlays*, Stockholm, Sweden, June 7–8, 2004, edited by Swedish Cement and Concrete Research Institute (CBI), RILEM PRO 43, 2004.
- 9. Hartl, G., Kraftverlauf in Beschichtungen, Zement und Beton, 28(2), 45–51, 1983 [in German].
- Hartl, G., Materialtechnologische Beurteilung von Verstärkungsmassnahmen, Beton und Stahlbetonbau 95(12), 707–712, 2000 [in German].

- 11. Beushausen, H., Long-term performance of bonded concrete overlays subjected to differential shrinkage, Ph.D. Thesis, University of Capetown, South Africa, 2005.
- 12. Beushausen, H. and Alexander, M., Bonded concrete overlays subjected to differential shrinkage An analytical model based on localized strain and stress. In *Proceedings International RILEM Workshop on Bonded Concrete Overlays*, Stockholm, Sweden, June 7–8, 2004, edited by Swedish Cement and Concrete Research Institute (CBI), RILEM PRO 43, 2004.
- Beushausen, H. and Alexander, M., Spannungen durch Verformungsbehinderung in gebundenen Aufbetonen, Beton und Stahlbetonbau 101(6), 394–401, 2006 [in German].
- 14. Beushausen, H. and Alexander, M., Localised strain and stress in bonded concrete overlays subjected to differential shrinkage, *Materials and Structures*, **40**(2), 189–199, 2007.
- 15. Jonasson, J.-E., Computer program for non-linear computations in concrete with regard to shrinkage, creep, and temperature. CBI Report No. 7:77, Swedish Cement and Concrete Research Institute, Stockholm. 161 pp., 1977 [in Swedish].
- 16. Haardt, P., Zementgebundene und kunststoffvergütete Beschichtungen auf Beton, Dissertation, Heft 13, TU Karlsruhe, 1991 [in German].
- 17. Silfwerbrand, J., Concrete overlays, Report No. 10, 3rd Edition, Chair of Structural Mechanics and Engineering, Department of Structural Engineering, Royal Institute of Technology, Stockholm, Sweden, 65 pp., 1997 [in Swedish].
- 18. Silfwerbrand, J., Effects of differential shrinkage, creep and properties of the contact surface on the strength of composite concrete slabs of old and new concrete. Bulletin No. 147, Department of Structural Mechanics and Engineering, Royal Institute of Technology, Stockholm, Sweden, 131 pp., 1987 [in Swedish].
- Beushausen, H. and Alexander, M., Failure mechanisms and tensile relaxation of bonded concrete overlays subjected to differential shrinkage, *Cement and Concrete Research*, 36, 1908–1914, 2007.
- 20. Huet, C., Adaptation d'un algorithme de Bazant au calcul des multilames visco-élastiques vieillissants, *Materials and Structures*, **13**(74), 91–98, 1980 [in French].
- Siestrunck, R., Lamer, P., Huet, C., and Alviset, L., Action de l'humidité sur la céramique envisagée dans le cadre de l'association béton-céramique. In Communication C.T.T.B. au Symposium Rilem/C.I.B., Helsinki, 1965 [in French].
- Gutsch, A. and Rostásy, F.S., Young concrete under high tensile stresses-creep relaxation and cracking. In *Proceedings RILEM Symposium on Thermal Cracking in Concrete at Early Ages*, R. Springenschmidt (Ed.), Chapman & Hall, London, pp. 111–116, 1995.
- 23. Horimoto, H. and Koyanagi, W., Estimation of stress relaxation in concrete at early ages. In *Proceedings RILEM Symposium on Thermal Cracking in Concrete at Early Ages*, R. Springenschmidt (Ed.), Chapman & Hall, London, pp. 95–102, 1995.
- Denarié, E., Cécot, C. and Huet, C., Characterization of creep and crack growth interactions in the fracture behaviour of concrete, Cement and Concrete Research, 36(3), 571–575, 2006.
- FIP, Federation Internationale de la Precontrainte, Structural Effects of Time-Dependent Behaviour of Concrete, Guide to Good Practice, FIP, Wexham Springs, 1982.
- Silfwerbrand, J., Composite action between partially chipped concrete bridge deck and overlay. Beam tests. Bulletin No. 142, Department of Structural Mechanics and Engineering, Royal Institute of Technology, Stockholm, Sweden, 72 pp., 1984 [in Swedish].
- Chausson, H., La durabilité des rechargements minces adhérents en béton renforcé de fibres métalliques. Doctoral Thesis, No. 2708, Université Paul Sabatier/LMDC, Toulouse, France, 1997 [in French].
- 28. RILEM TC-119-TCE, Avoidance of thermal cracking in concrete at early ages TCE3: Testing of the cracking tendency of concrete at early ages using the cracking frame test, *Materials and Structures*, **30**, 461–464, 1997.
- 29. Kovler, K., Testing system for determining the mechanical behaviour of early age concrete under restrained and free shrinkage, *Materials and Structures*, **27**, 324–330, 1994.
- Bjontegaard, O., Thermal dilatation and autogenous deformation as driving forces to selfinduced stresses in high performance concrete, Doctoral Thesis, Trondheim, Norway 1999.

31. Pigeon, M., Toma, G., Delagrave, A., Bissonnette, B., Marchand, J., and Prince, J.C., Equipement for the analysis of the behaviour of concrete under restrained shrinkage at early ages, *Magazine of Concrete Research*, **52**(4), 497–502, 2000.

- Altoubat, S.A. and Lange, D.A., Tensile basic creep: Measurements and behavior at early age, ACI Materials Journal, 95(5), 386–393, 2001.
- 33. Bentur, A. and Kovler, K., Evaluation of early-age cracking characteristics in cementitious systems, *Materials and Structures*, **36**, 183–190, 2003.
- 34. Charron, J-P., Contribution à l'étude du comportement au jeune âge des matériaux cimentaires en conditions des déformations libre et restreinte. Ph.D. Thesis, University Laval, Quebec, Canada, 2003 [in French].
- 35. Sule, M., Effect of reinforcement on early-age cracking in high strength concrete, Ph.D. Thesis, TU Delft, 2003.
- Kamen, A., Denarié, E., and Brühwiler E., Mechanical behaviour of ultra high performance fibre reinforced concretes (UHPFRC) at early age, and under restraint. In *Proceedings CON-CREEP 7*, G. Pijaudier-Cabot, B. Gérard, and P. Acker (Eds.), Hermès Publishing, pp. 591– 596, 2005.
- Martinola, G., Rissbildung und Ablösung zementgebundener Beschichtungen auf Beton. Dissertation. ETH Zürich, Switzerland, No. 13520, 2000 [in German].
- 38. Bernard, O. and Brühwiler, E., The influence of reinforcement in the new layer on hygral cracking in composite structural elements, *Materials and Structures*, **36**, 118–126, 2003.
- 39. Bernard, O. and Brühwiler, E., Influence of autogenous shrinkage on early age behaviour of structural elements consisting of concretes of different ages, *Materials and Structures*, **35**, 550–556, 2002.
- Roelfstra, P.E., Salet, A.M., and Kuiks, J.E., Defining and application of stress-analysis-based temperature difference limits to prevent early-age cracking in concrete structures. In *Proceedings No. 25 of the International RILEM Symposium: Thermal Cracking in Concrete at Early Age*, Münich, pp. 273–280, 1994.
- Habel, K., Structural behaviour of elements combining ultra-high performance fibre reinforced concretes (UHPFRC) and reinforced concrete. Doctoral Tthesis No. 3036, Ecole Polytechnique Fédérale de Lausanne, Lausanne, Switzerland, 2004.
- 42. Habel, K., Denarié, E., and Brühwiler, E., Time dependent behaviour of elements combining UHPFRC and concrete, *Materials and Structures*, **39**, 557–569, 2006.
- Martinola, G., Sadouki, H., and Wittmann, F.H., Numerical model for minimizing the risk of damage in repair system, ASCE Journal of Materials in Civil Engineering, 121–129, 2001.
- 44. DIANA, User's manual-release 6.1, Diana Analysis BV, Delft, the Netherlands, 1996.
- 45. Laurence, O., La fissuration due au retrait restreint dans les réparations minces en béton: Apports combinés de l'expérimentation et de la modélisation, Doctoral Thesis, Ecole Nationale des Ponts et Chaussées, Paris, France, 2001 [in French].
- Tran, Q.T., Toumi, A., and Granju, J-L., Experimental and numerical investigation of the debonding interface between an old concrete and an overlay, *Materials and Structures*, 39(3), 379–389, 2006.
- 47. Féron, C., Etude des mécanismes de generation de contraintes et de fissuration par retrait gêné dans les structures à base de matériaux cimentaires, Doctoral Thesis, Institut National des Sciences Appliqués de Lyon, No. 2002 ISAL 0025, 2002 [in French].
- McCullough, B.F. and Rasmussen, R.O., Fast-track paving: Concrete temperature control and traffic opening criteria for bonded concrete overlays. Volume I: Final report, Federal Highway Administration Report FHWA-RD-98-167, Washington, USA, 1999.
- McCullough, B.F. and Rasmussen, R.O., Fast-track paving: Concrete Temperature Control and Traffic Opening Criteria for Bonded Concrete Overlays Volume II: HIPERPAV User's Manual, Federal Highway Administration Report FHWA-RD-98-168, Washington, USA, 1999.
- Rasmussen, R.O., et al., Fast-track paving: Concrete temperature control and traffic opening criteria for bonded concrete overlays. Volume III: Addendum to the HIPERPAV user's manual, Federal Highway Administration Report FHWA-RD-99-200, Washington, 1999.

51. Rasmussen, R.O., McCullough, B.F., and Weissmann, J., Development of a bonded concrete overlay computer-aided design system, Research Report No. 2911-1, Centre for Transportation Research, The University of Texas at Austin, 1995.

52. Rostasy, F.S., Kraus, M., and Budelmann, H., Planungswerkzeug zur Kontrolle der frühen Rissbildung in massigen Betonbauteilen – Teil 5: Behinderung und Zwang, *Bautechnik* **79**(11), 778–789, 2002 [in German].